

This article was downloaded by: [Ferdowsi University]

On: 11 February 2012, At: 23:06

Publisher: Taylor & Francis

Informa Ltd Registered in England and Wales Registered Number: 1072954 Registered office: Mortimer House, 37-41 Mortimer Street, London W1T 3JH, UK



Mechanics Based Design of Structures and Machines: An International Journal

Publication details, including instructions for authors and subscription information:

<http://www.tandfonline.com/loi/lmbd20>

Timestep Selection for Dynamic Relaxation Method

M. Rezaiee-Pajand^a, M. Kadkhodayan^b & J. Alamatian^c

^a Department of Civil Engineering, Ferdowsi University of Mashhad, Mashhad, Iran

^b Department of Mechanical Engineering, Ferdowsi University of Mashhad, Mashhad, Iran

^c Department of Civil Engineering, Mashhad Branch, Islamic Azad University, Mashhad, Iran

Available online: 10 Jan 2012

To cite this article: M. Rezaiee-Pajand, M. Kadkhodayan & J. Alamatian (2012): Timestep Selection for Dynamic Relaxation Method, *Mechanics Based Design of Structures and Machines: An International Journal*, 40:1, 42-72

To link to this article: <http://dx.doi.org/10.1080/15397734.2011.599311>

PLEASE SCROLL DOWN FOR ARTICLE

Full terms and conditions of use: <http://www.tandfonline.com/page/terms-and-conditions>

This article may be used for research, teaching, and private study purposes. Any substantial or systematic reproduction, redistribution, reselling, loan, sub-licensing, systematic supply, or distribution in any form to anyone is expressly forbidden.

The publisher does not give any warranty express or implied or make any representation that the contents will be complete or accurate or up to date. The accuracy of any instructions, formulae, and drug doses should be independently verified with primary sources. The publisher shall not be liable for any loss, actions, claims, proceedings, demand, or costs or damages whatsoever or howsoever caused arising directly or indirectly in connection with or arising out of the use of this material.

TIMESTEP SELECTION FOR DYNAMIC RELAXATION METHOD[#]

M. Rezaiee-Pajand¹, M. Kakhodayan², and J. Alamatian³

¹Department of Civil Engineering, Ferdowsi University of Mashhad, Mashhad, Iran

²Department of Mechanical Engineering, Ferdowsi University of Mashhad, Mashhad, Iran

³Department of Civil Engineering, Mashhad Branch, Islamic Azad University, Mashhad, Iran

This paper focuses on the dynamic relaxation (DR) method as an efficient approach for solving a system of simultaneous equations. This is an iterative procedure which can be used for both finite element and finite difference structural analysis. The DR method has a simple algorithm. However, it suffers from low convergence rate. In the current study, a residual energy minimizer timestep (REMT) will be formulated by minimizing the residual energy. A variety of structural analyses with linear and nonlinear (elastic large deflection) behaviors demonstrate the potential of the proposed strategy. The results indicate that the REMT improves the convergence rate of DR without any additional constraints so that the cost and computational time are decreased.

Keywords: Convergence rate; Dynamic relaxation; Nonlinear analysis; Residual energy minimizer timestep.

INTRODUCTION

Finite element or finite difference applications to an analytical model of complex structures lead to a system of simultaneous equations, which can approximate the behavior of the system. The force displacement relationship may be written as:

$$\mathbf{SD} = \mathbf{P}, \quad (1)$$

where \mathbf{S} is the stiffness matrix and \mathbf{D} and \mathbf{P} are nodal displacements and equivalent nodal forces, respectively. Whenever analysis assumptions are very close to the real conditions, results will be more accurate and show more conformity with the available experimental data. For example, nonlinear effects such as elastic-plastic or large deformation behaviors lead to a complex system of equations. In this case, the stiffness matrix or even the external load vector will be a function of displacement,

Received July 5, 2010; Accepted June 13, 2011

[#]Communicated by G. Hulbert.

Correspondence: M. Rezaiee-Pajand, Department of Civil Engineering, Ferdowsi University of Mashhad, Mashhad, Iran; E-mail: mrpajand@yahoo.com

Eq. (1) will be nonlinear. By solving this equation, displacement vector is calculated and other quantities such as strains and stresses will be calculated explicitly based on the displacements. Therefore, the final stage of each analysis is completed by employing an equation solver. For instance, the dynamic relaxation (DR) method is a powerful procedure which has been used in a variety of engineering analyses, such as frames, trusses, plates and shells.

DR, was introduced by Otter (Otter, 1966) or Day (Day, 1965), is an iterative technique and can be utilized for solving a system of linear and nonlinear simultaneous equations. This procedure may be explained by either mathematical or physical theories. Mathematically, DR formulation is based on the second-order Richardson rule, developed by Frankel (Frankel, 1950). The heat transition problem in a rectangular region is an example of this formulation. Physically, the DR scheme can be illustrated by the steady state response of an artificial dynamic system with fictitious density. This kind of formulation was introduced by (Welsh, 1967) and (Cassell et al., 1968).

The DR method has been used in nonlinear problems (Rushton, 1968) and its formulation can be derived from the first order dynamic equilibrium relationship (Brew and Brotton, 1972). In the elementary approaches, the fictitious mass has been defined by using the upper bound of the spectral radius of the coefficient's matrix (Wood, 1971). An estimation of the critical damping was also obtained by Bunce (1972). Alwar and his coworkers determined the steady-state response from an exponential function (Alwar et al., 1975). Furthermore, Cassell and Hobbs utilized Gerschgorin theory for fictitious mass values and applied this method to nonlinear problems (Cassell and Hobbs, 1976).

In other applications, the DR algorithm has been utilized for nonlinear analysis of plates (Frieze et al., 1978). The first error analysis of DR iterations was performed by Papadrakakis, who described an automatic procedure for the selection of DR parameters (Papadrakakis, 1981). Moreover, Underwood presented another interesting formulation for the explicit DR method (Underwood, 1983). The implicit DR method has also been formulated by Felippa (1982). Zienkiewicz et al. suggested an accelerated procedure for the improvement of the convergence rate (Zienkiewicz and Lohner, 1985). By using weighted factors for mass and damping of each degree of freedom, DR has been used in finite element analysis for bending plates (Shawi and Mardirosion, 1987). Moreover, fictitious time and damping can be determined by Rayleigh's principle (Qiang, 1988). In another study, the maDR algorithm was proposed in which the estimation of steady-state response was modified (Zhang and Yu, 1989).

Other researchers have used the DR algorithm for different engineering problems Turvey and Salehi, 1990; Bardet and Proubet, 1991. The first use of DR scheme in the post-buckling analysis was performed by Ramesh and Krishnamoorthy, in which they independently combined the DR algorithm with the incremental displacement approach and arc length procedure (Ramesh and Krishnamoorthy, 1993, 1994). In another study, new models were introduced for fictitious damping (Zhang et al., 1994). Moreover, applications of DR method in elastic-plastic and buckling problems have been studied for plate structures (Kadkhodayan and Zhang, 1995; Kadkhodayan et al., 1997). By using DR method, a nonlinear analysis of buckling propagation in pipelines has been studied (Pasqualino and Estefan, 2001). Furthermore, a shape-finding analysis was

performed by the DR algorithm (Wood, 2002; Han and Lee, 2003). Besides, the DR method has been combined with neural networks to increase model accuracy of tensegrity structures (Domer et al., 2003). It was also successfully applied to linear and nonlinear analysis of composite structures (Turvey and Salehi, 2005). Recently, a modified fictitious timestep has been formulated based on minimization of the residual force in each DR iteration (Kadkhodayan et al., 2008). Moreover, the DR method has an ability to be used in the nonlinear dynamic analysis of structures (Rezaiee-Pajand and Alamatian, 2008a,b). Recently, some new formulations have been proposed for viscous DR parameters (Rezaiee-Pajand and Alamatian, 2010; Rezaiee-Pajand et al., 2011). In the latest study, the structures with snap-through and snap-back behaviors have been analyzed with DR procedure, successfully (Rezaiee-Pajand and Alamatian, 2011).

The aim of this paper is to improve the convergence rate of DR method by defining a new energy criterion. First, the explicit formulation of DR is reviewed. Then, a new fictitious timestep is formulated by defining and minimizing of an energy function. For numerical verification, some linear and nonlinear (elastic large deflection) structures are analyzed by utilizing the finite elements and finite differences techniques along with the suggested formulations.

DR METHOD

Both mathematical and physical concepts are utilized in DR formulation. According to the DR method, an equivalent static system, Eq. (1), is shifted to an assumed dynamic space by adding artificial inertia and damping forces, as follows:

$$\mathbf{M}^n \mathbf{A}^n + \mathbf{C}^n \mathbf{V}^n + \mathbf{S}^n \mathbf{D}^n = \mathbf{P}^n, \quad (2)$$

where \mathbf{V}^n and \mathbf{A}^n are the artificial velocity and acceleration vectors, and \mathbf{M}^n and \mathbf{C}^n are the fictitious mass and damping matrices in the n th iteration of DR, respectively. The steady-state response of this artificial dynamic system is the solution of Eq. (1), when the fictitious velocities and accelerations become zero. There are different approaches to derive the DR iterative relationships. In a common formulation, such as the Papadrakakis scheme or Underwood procedure, mass and damping matrices are assumed to be diagonal and the explicit central finite difference integration is used. Consequently, the following DR iterative relationships are obtained (Underwood, 1983):

$$\mathbf{V}^{n+\frac{1}{2}} = \frac{2 - c^n \tau^n}{2 + c^n \tau^n} \mathbf{V}^{n-\frac{1}{2}} + \frac{2\tau^n}{2 + c^n \tau^n} \frac{1}{m_{ii}} \mathbf{M}^{-1} \mathbf{R}^n \quad (3)$$

$$\mathbf{D}^{n+1} = \mathbf{D}^n + \tau^{n+1} \mathbf{V}^{n+\frac{1}{2}}, \quad (4)$$

where τ^n is the fictitious timestep and number of degrees of freedom, respectively. In the explicit DR procedure introduced by Underwood, c^n is damping factor in the n th DR iteration and is defined as below (Underwood, 1983):

$$\mathbf{C}^n = c^n \mathbf{M}^n. \quad (5)$$

The residual force in the n th iteration of DR scheme may also be written as:

$$\mathbf{R}^n = \mathbf{P} - \mathbf{f}^n, \quad (6)$$

where \mathbf{f}^n is the internal force vector in n th DR iteration, which is formulated from the fundamental structural analysis relationships.

Other quantities for explicit DR formulation were also proposed by Papadrakakis (Papadrakakis, 1981). In the explicit DR, fictitious mass, damping factor and timestep are defined so that the stability is guaranteed and the convergence rate reaches to its maximum value. For this purpose, the Gerschgorin's circle theory and Rayleigh's principle are used for artificial mass matrix and damping factor as follows (Underwood, 1983; Zhang et al., 1994):

$$m_{ii}^n > \frac{(\tau^n)^2}{4} \sum_{j=1}^{\text{DOF}} |s_{ij}| \quad i = 1, 2, \dots, \text{DOF} \quad (7)$$

$$c^n = 2 \sqrt{\frac{(\mathbf{D}^n)^T \mathbf{S}^n \mathbf{D}^n}{(\mathbf{D}^n)^T \mathbf{M}^n \mathbf{D}^n}}. \quad (8)$$

Here DOF is number of degree of freedom. It should be noted that the numerical stability of DR iterations is guaranteed by mathematical theories (Gerschgorin's circle theory). Moreover, physical concepts such as critical damping theory may be used to improve the convergence rate of DR method (Rayleigh's principle). Some researchers also proposed using an individual damping factor for each node (Kadkhodayan et al., 1997). In the most common DR algorithms, constant fictitious time (CFT) is used ($\tau = 1$), however, there are some procedures for automatic selection of the timestep (Qiang, 1988).

Generally, it is possible in the DR formulation to categorize unknown parameters into two different groups based on their specifications. For instance, the numerical stability and the convergence rate are the most important specifications in the first and second groups of parameters, respectively. In the explicit DR formulation, the fictitious mass has the most significant role to guarantee the stability of the procedure. Therefore, this parameter has to be calculated so that a steady-state response is obtained. On the other hand, the fictitious damping factor and the timestep control the convergence rate of DR iterations, hence, it would be reasonable to seek for a new fictitious timestep so that a better convergence rate is obtained. Based on the vital specifications of DR method, two fundamental criteria for this purpose may be applied, i.e. the out-of-balance force and the residual energy. The first one, which was previously suggested by the authors, is based on the minimization of the out-of-balance force. The basic formulation of this procedure is described briefly here after. The out-of-balance force function is defined as follows:

$$\text{UBF} = (\mathbf{R}^{n+1})^T \cdot \mathbf{R}^{n+1}, \quad (9)$$

where UBF is the norm of the unbalance force vector in the $n + 1$ th iteration of DR method. By utilizing a central finite difference approach, the out-of-balance force can be written as below:

$$\mathbf{R}^{n+1} = \mathbf{R}^n + \tau^{n+1} \dot{\mathbf{R}}^{n+\frac{1}{2}}. \quad (10)$$

In this equation, $\dot{\mathbf{R}}^{n+\frac{1}{2}}$ is the rate of out-of-balance force vector. According to the following relation, this quantity can be formulated by deriving Eq. (6) with respect to the fictitious time:

$$\dot{\mathbf{R}}^{n+\frac{1}{2}} = \frac{d}{d\tau} \left(\mathbf{R}^{n+\frac{1}{2}} \right) = \frac{d}{d\tau} \left(\mathbf{P} - \mathbf{f}^{n+\frac{1}{2}} \right) = \frac{d\mathbf{P}}{d\tau} - \frac{d\mathbf{f}^{n+\frac{1}{2}}}{d\tau} = -\dot{\mathbf{f}}^{n+\frac{1}{2}}, \quad (11)$$

where $\dot{\mathbf{f}}^{n+\frac{1}{2}}$ is the rate of internal force vector. It should be noted that during the DR iteration, the external force is kept constant; that is, $\frac{d\mathbf{P}}{d\tau} = 0$. By substituting Eq. (11) into Eq. (10), the out-of-balance force is obtained in the following form:

$$\mathbf{R}^{n+1} = \mathbf{R}^n - \tau^{n+1} \dot{\mathbf{f}}^{n+\frac{1}{2}}. \quad (12)$$

Moreover, the rate of external force vector ($\dot{\mathbf{f}}^{n+\frac{1}{2}}$) can be found by using the chain rule of differentiation as follows (Kadkhodayan et al., 2008):

$$\dot{f}_i^{n+\frac{1}{2}} = \sum_{j=1}^{\text{DOF}} s_{ij,T}^{n+\frac{1}{2}} v_j^{n+\frac{1}{2}}. \quad (13)$$

Because it is usually difficult to determine the tangent stiffness matrix at the middle of each iteration, as required in Eq. (13), it would be more practical to use the value obtained in the previous iteration. In this case, the following approximate relation may be used:

$$\dot{f}_i^{n+\frac{1}{2}} \approx \sum_{j=1}^{\text{DOF}} s_{ij}^n v_j^{n+\frac{1}{2}} \quad i = 1, 2, \dots, \text{DOF} \quad (14)$$

Now, if the unbalance force function is minimized, a modified fictitious time (MFT) can be obtained (Kadkhodayan et al., 2008):

$$\frac{\partial \text{UBF}}{\partial \tau^{n+1}} = 0 \Rightarrow \tau_{\text{MFT}} = \frac{(\mathbf{R}^n)^T \cdot \dot{\mathbf{f}}^{n+\frac{1}{2}}}{\left(\dot{\mathbf{f}}^{n+\frac{1}{2}} \right)^T \cdot \dot{\mathbf{f}}^{n+\frac{1}{2}}} = \frac{\sum_{i=1}^{\text{DOF}} r_i^n \dot{f}_i^{n+\frac{1}{2}}}{\sum_{i=1}^{\text{DOF}} \left(\dot{f}_i^{n+\frac{1}{2}} \right)^2}. \quad (15)$$

By using the second derivative test, it can be proven mathematically that the above timestep minimizes the out-of-balance force function in each iteration of the DR method. Therefore, the convergence rate will increase, and the analysis time will decrease. In the next part, the second criterion based on the residual energy is proposed and a new technique for calculating the fictitious timestep is suggested.

RESIDUAL ENERGY CRITERION

The work or energy quantity is one of the most powerful parameters that may be used in the investigation of a physical phenomenon. Simplicity and higher efficiency are the main advantages of any algorithm, which is based on work and energy formulation. There are many applications of work quantities in structural engineering, such as the study of stability conditions and structural analysis formulation. In this section, an out-of-balance energy criterion will be utilized for the more suitable convergence rate of the DR method.

Kinetic energy is constructed based on two parameters: the displacement increment, which may be noted as residual displacement, and the residual force. In the steady state response, the out-of-balance force and displacement increment (velocity) become zero. The suitable convergence rate of DR iterations will be obtained if both residual force and residual displacement have a maximum reduction, simultaneously.

It is important to note that, based on Eq. (3), the displacement increment ($\tau^{n+1}V^{n+\frac{1}{2}}$) is a function of two parameters: residual force of the current step and the velocity of the previous timestep. Assume that the residual force of the current timestep has been minimized; but there is a velocity from the previous timestep which has not taken into account. In this case (MFT), both the residual force and displacement are not minimized at the same time. This residual displacement provides residual force in the next timestep. According to this discussion, the more suitable approach is the one in which both residual force and displacement have been minimized, simultaneously. In this study, residual energy of the structure is a function of the residual force and displacement vectors. The unbalance energy function can be defined as follows,

$$UBE = \sum_{i=1}^{DOF} (\delta D_i^{n+1} r_i^{n+1})^2, \quad (16)$$

where UBE is the unbalance energy function in the $n+1$ th iteration of the DR process. If the out-of-balance force is replaced from Eq. (12), unbalance energy function becomes,

$$UBE = (\tau^{n+1})^2 \sum_{i=1}^{DOF} \left(v_i^{n+\frac{1}{2}} (r_i^n - \tau^{n+1} \dot{f}_i^{n+\frac{1}{2}}) \right)^2. \quad (17)$$

The necessary condition for minimization of the unbalance energy function is that the first order derivative of Eq. (17) with respect to the fictitious timestep is equal to zero. This procedure leads to the second order equation as follows,

$$\frac{\partial UBE}{\partial \tau^{n+1}} = 0 \Rightarrow A_1^{n+1} (\tau^{n+1})^2 + A_2^{n+1} \tau^{n+1} + A_3^{n+1} = 0, \quad (18)$$

where A_1^{n+1} , A_2^{n+1} and A_3^{n+1} are constant factors and can be found as below:

$$A_1^{n+1} = 2 \sum_{i=1}^{DOF} \left(v_i^{n+\frac{1}{2}} \dot{f}_i^{n+\frac{1}{2}} \right)^2 \quad (19)$$

$$A_2^{n+1} = -3 \sum_{i=1}^{DOF} \left[\left(v_i^{n+\frac{1}{2}} \right)^2 r_i^n \dot{f}_i^{n+\frac{1}{2}} \right] \quad (20)$$

$$A_3^{n+1} = \sum_{i=1}^{DOF} \left(v_i^{n+\frac{1}{2}} r_i^n \right)^2. \quad (21)$$

If the discriminate of Eq. (18) is equal to or greater than zero, the following two values are calculated for the residual energy minimizer timestep (REMT):

$$\tau_{\text{REMT}}^{n+1} = \frac{-A_2^{n+1} \pm \sqrt{(A_2^{n+1})^2 - 4A_1^{n+1}A_3^{n+1}}}{2A_1^{n+1}}. \quad (22)$$

The sufficient condition for minimization of the UBE function is that the second order derivative of this function be greater than zero:

$$\frac{\partial^2 \text{UBE}}{\partial (\tau^{n+1})^2} > 0 \Rightarrow 2A_1^{n+1} \tau^{n+1} + A_2^{n+1} > 0. \quad (23)$$

It is clear that minimization of the out-of-balance energy function is conditional. If the discriminant of Eq. (18) is smaller than zero, the necessary condition for minimization will not be available. On the other hand, selection of the timestep between two values of Eq. (22) is taken so that condition (23) is satisfied. For more clarification, proposed timestep is simplified for a single degree of freedom system (DOF = 1). In this case, the quantities A_1^{n+1} , A_2^{n+1} and A_3^{n+1} are as follows:

$$A_1^{n+1} = 2\left(v^{n+\frac{1}{2}} \dot{f}^{n+\frac{1}{2}}\right)^2 \quad (24)$$

$$A_2^{n+1} = -3\left(v^{n+\frac{1}{2}}\right)^2 r^n \dot{f}^{n+\frac{1}{2}} \quad (25)$$

$$A_3^{n+1} = \left(v^{n+\frac{1}{2}} r^n\right)^2. \quad (26)$$

Substituting Eqs. (24), (25), and (26) into Eq. (22), two timesteps are obtained:

$$\tau_1^{n+1} = \frac{r^n}{\dot{f}^{n+\frac{1}{2}}} \quad (27)$$

$$\tau_2^{n+1} = \frac{r^n}{2\dot{f}^{n+\frac{1}{2}}}. \quad (28)$$

By replacing these timesteps in Eq. (23) and using Eq. (14) following result is obtained:

$$\frac{\partial^2 \text{UBE}}{\partial (\tau_1^{n+1})^2} = s^n \left(v^{n+\frac{1}{2}}\right)^2 r^n v^{n+\frac{1}{2}} \quad (29)$$

$$\frac{\partial^2 \text{UBE}}{\partial (\tau_2^{n+1})^2} = -s^n \left(v^{n+\frac{1}{2}}\right)^2 r^n v^{n+\frac{1}{2}} \quad (30)$$

which s^n is tangent stiffness of the single degree of freedom system and is positive. Based on Eq. (3), positive residual force, r^n , creates a positive velocity ($v^{n+\frac{1}{2}}$). Therefore, the residual force and velocity have the same sign. This is the sign that the second order derivative in Eq. (29) will be positive. As a result, τ_1^{n+1} (from Eq. (27)), which is corresponding to Eq. (29) minimizes the residual energy of a single degree of freedom system.

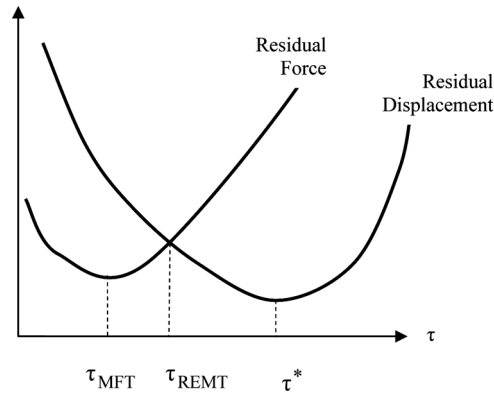


Figure 1 Schematic variation of out-of-balance force and residual displacement.

Although both MFT and REMT algorithms have the same mathematical convergence ranks (see the appendix), the new proposed algorithm is more powerful and could reach better convergence. It should be pointed out that the minimums of the out-of-balance force and out-of-balance displacement do not take place concurrently. Figure 1 displays such a behavior schematically, where variations of these two are plotted against the fictitious timestep. For instance, the minimum values of the unbalance force and residual displacement happen in the timesteps τ_{MFT} and τ^* , respectively. If the minimum unbalance force criterion is utilized, the fictitious timestep τ_{MFT} will be obtained. In this case, the residual displacement is far from its minimum value. Hence, it won't be the best selection because the residual displacement of the current iteration creates a bigger out-of-balance force in the next step. There is a similar situation for the timestep τ^* . However, using the minimum unbalance energy criterion gives the fictitious timestep as τ_{REMT} . As a result, it would be reasonable to accept that the minimum unbalance energy criterion be more efficient than the other methods.

THE DR ALGORITHM USING REMT

By using the proposed formulation, a DR method with better convergence rate is obtained. This algorithm is based on the minimization of the unbalance energy function. If the UBE function cannot be minimized, then the fictitious timestep will be calculated by minimizing the out-of-balance force (UBF). The proposed algorithm is presented in the following.

- (a) Assume values for initial fictitious velocity (null vector), initial displacement (null vector or convergence displacement on the previous increment, if available), fictitious timestep (1) and a convergence criterion for the out-of-balance force and kinetic energy ($e_R = 1.0E - 6$ and $e_K = 1.0E - 12$),
- (b) construct tangent stiffness matrix and internal force vector,
- (c) calculate out-of-balance force vector using Eq. (6),
- (d) if $\|\mathbf{R}^n\| \leq e_R$, go to (s), otherwise continue,
- (e) construct fictitious diagonal mass matrix using Eq. (7),

- (f) calculate fictitious damping factor by Eq. (8),
- (g) update fictitious velocity vector using Eq. (3),
- (h) if $\|\mathbf{V}^{n+\frac{1}{2}}\| \leq e_K$, go to (s), otherwise, continue,
- (i) determine internal force increment vector by Eq. (14),
- (j) calculate A_1^{n+1} , A_2^{n+1} and A_3^{n+1} by Eqs. (19), (20), and (21), respectively,
- (k) if $(A_2^{n+1})^2 - 4A_1^{n+1}A_3^{n+1} < 0$, go to (p), otherwise continue,
- (l) calculate two fictitious timesteps (τ_1^{n+1} , τ_2^{n+1}) from Eq. (22),
- (m) find $\text{UBE}(\tau_1^{n+1})$ and $\text{UBE}(\tau_2^{n+1})$ by using τ_1^{n+1} and τ_2^{n+1} in Eq. (17),
- (n) if $\text{UBE}(\tau_1^{n+1}) > \text{UBE}(\tau_2^{n+1})$ then $\tau_{\text{REMT}} = \tau_1^{n+1}$, otherwise, $\tau_{\text{REMT}} = \tau_2^{n+1}$,
- (o) go to (q),
- (p) calculate fictitious timestep by Eq. (15), τ_{MFT} ,
- (q) update displacement vector using Eq. (4),
- (r) go to (b),
- (s) print results of the current increment,
- (t) if increments are not complete, go to (a), otherwise, stop.

As it mentioned, the proposed algorithm transforms to the MFT method when the unbalance energy function does not have any minimum. As a result, the MFT technique is a special case of the proposed algorithm (REMT).

NUMERICAL EXAMPLES AND DISCUSSION

In this part, the ability of the proposed REMT algorithm is investigated during analysis by some numerical examples. To show the preference of the new method, the obtained results are compared with those from CFT (constant fictitious time) and MFT (modified fictitious time) algorithms. The mentioned three techniques are utilized to analyze some frame, truss, plate and shell structures with small and large deformation behaviors. Finite element and finite difference formulations are considered and a computer program (written by the authors) is utilized for all numerical studies. The nonlinear analyses are based on elastic large deflection behavior.

Space Truss

Figure 2 displays a space truss with axial rigidity $AE = 10,000 \text{ N}$ (Saka, 1990). Because of its symmetrical geometry and loading, this structure has only one effective degree of freedom (displacement in the Z direction i. e. D). A total Lagrangian finite element approach is used for its elastic-large deformation formulation (Felippa, 1997). The internal force and tangent stiffness relationships for linear and nonlinear analyses can be formulated as follows;

$$f(D) = 2 \frac{AE}{L_0^3} (D^2 + 2Z_0D)(D + Z_0) \quad \text{Non-linear Elastic Large Deflection} \quad (31)$$

$$S_T = 2 \frac{AE}{L_0^3} [2(D + 2Z_0)^2 + (D^2 + 2Z_0D)]$$

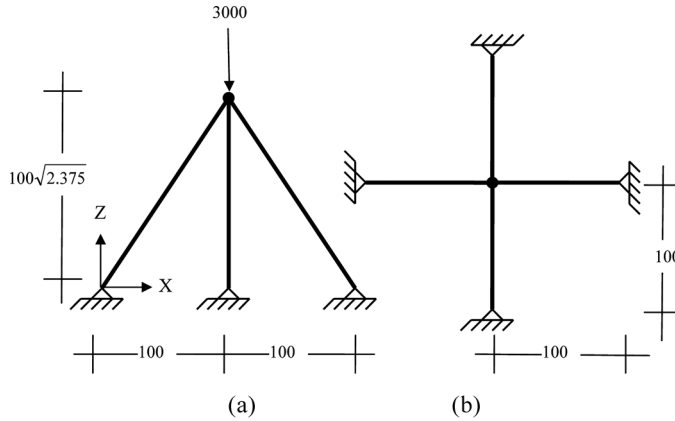


Figure 2 Space truss: (a) side view, (b) top view (dimensions in millimeters).

$$f(D) = 4 \frac{AE}{L_0^3} Z_0^2 D$$

Linear Elastic Small Deflection (32)

$$S_T = 4 \frac{AE}{L_0^3} Z_0^2$$

Here L_0 and Z_0 are original the length of each member and the height of the tip node in undeformed truss ($100\sqrt{2.375}$ mm), respectively. Figure 3 shows the load deflection curves for both linear and nonlinear analyses. In the nonlinear analysis (elastic large deflection), the softening behavior occurs. The number of required iterations for the convergence algorithms has also been inserted in Table 1. Using linear analysis, the MFT and REMT methods converge to the solution after only one iteration. This means that the convergence rate of the suggested technique is infinite in linear behavior as is proved mathematically in the appendix. It may also be easily observed in other linear systems with a single degree of freedom.

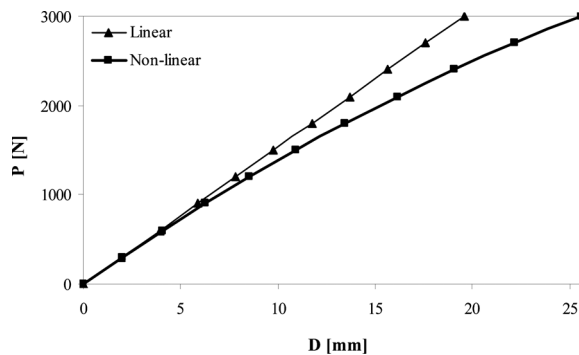


Figure 3 Load-deflection curves for space truss.

Table 1 The number of iterations for convergence in the space truss

Analysis	Meth.	Number of iterations for each load increment										Improvement (%)		
		1	2	3	4	5	6	7	8	9	10	Total	$\frac{\text{CFT-REMT}}{\text{CFT}}$	$\frac{\text{MFT-REMT}}{\text{MFT}}$
Linear	CFT	20	19	19	19	19	19	19	19	19	19	195	98.9	-
	MFT	5	4	4	4	4	4	4	4	4	4	1		
	REMT	2	2	2	2	2	2	2	2	2	2	20		
Nonlinear	CFT	20	19	19	20	20	21	21	22	22	22	209	97.0	6.1
	MFT	7	7	9	2	5	8	2	6	1	8	5		
	REMT	6	6	6	6	6	6	6	8	8	8	66		
	REMT	6	6	6	6	6	6	6	6	6	62			

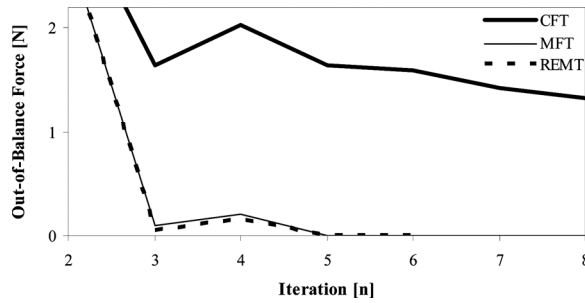


Figure 4 Variation of out-of-balance force for the 10th increment of non-linear space truss.

On the other hand, the REMT algorithm causes a maximum reduction in convergence rate up to about 95% and 5% in comparison to the CFT and MFT methods, respectively. Therefore, the proposed scheme has higher efficiency than the both previous techniques, especially in the nonlinear analysis. The variations of unbalance force and kinetic energy have been plotted in Figs. 4 and 5, respectively for 10th increment of the nonlinear analysis. These Figures show that using REMT reduces the out-of-balance force and the kinetic energy quicker than when the MFT and constant fictitious time is used.

Truss-Spring System

Figure 6 shows a nonlinear system with one degree of freedom. This structure is formed by a spring with stiffness $K_s = 10.51 \text{ N/cm}$ and a truss element with axial rigidity $AE = 44483985.77 \text{ N}$. The fundamental relationships for internal force (f) and tangent stiffness (S_T) are as follow, (Underwood, 1983),

$$f(D) = 0.5AE(\cos^2 \phi) \left(\frac{D}{L_0} \right)^2 \left[\frac{D}{L_0} \cos^2 \phi - 3 \sin \phi \right] + k_s D + \left(\frac{AE D}{L_0} \right) \sin^2 \phi \quad (33)$$

$$S_T = 1.5AE(\cos^2 \phi) \left[\frac{D}{L_0} \cos^2 \phi - 2 \sin \phi \right] \left(\frac{D}{L_0^2} \right) + k_s + \frac{AE \sin^2 \phi}{L_0} \quad (34)$$

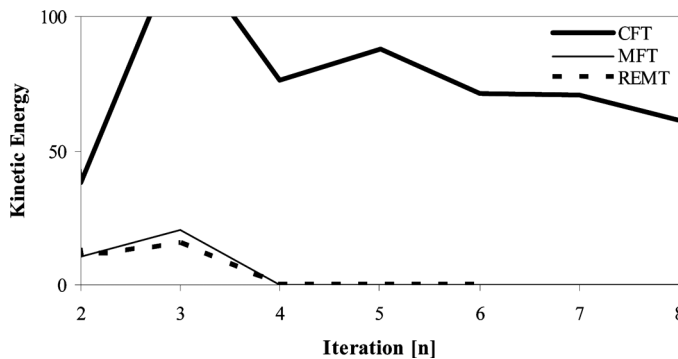


Figure 5 Variation of kinetic energy for the 10th increment of non-linear space truss.

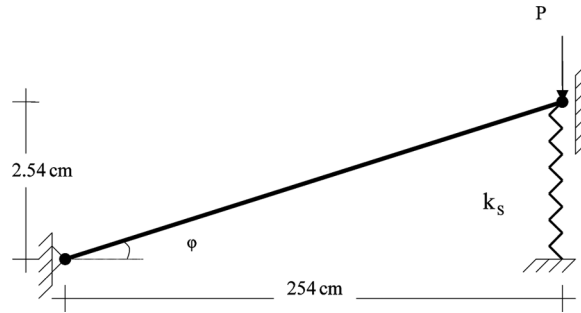


Figure 6 Truss-spring system.

The loading process is completed in twelve increments with each load step of 4.4484 N. Figure 7 displays the load-deflection curve for this system. This structure has both softening and hardening behaviors. The number of required iterations for convergence has also been inserted in Table 2. When the REMT is used, the maximum reduction in comparison to the MFT and CFT algorithms is up to 90% and 5%, respectively. On the other hand, Figs. 8 and 9 demonstrate variations of out-of-balance force and kinetic energy, respectively for the 12th increment. From these figures, one can clearly observe that using REMT reduces the out-of-balance force and the kinetic energy quicker than those when MFT and CFT methods are employed.

LINEAR 2D TRUSS

Figure 10 shows a 2D truss which has two degrees of freedom. By considering the elastic linear small deflection behavior ($AE = 617, 511, 452 \text{ N}$), the governing equilibrium equations form a system of two coupled linear algebraic equations as follows;

$$\begin{bmatrix} 173.80127 & 31.41756 \\ 31.41756 & 273.62511 \end{bmatrix} \begin{Bmatrix} D_x \\ D_y \end{Bmatrix} = \begin{Bmatrix} 5 \\ -50 \end{Bmatrix} MN. \quad (35)$$

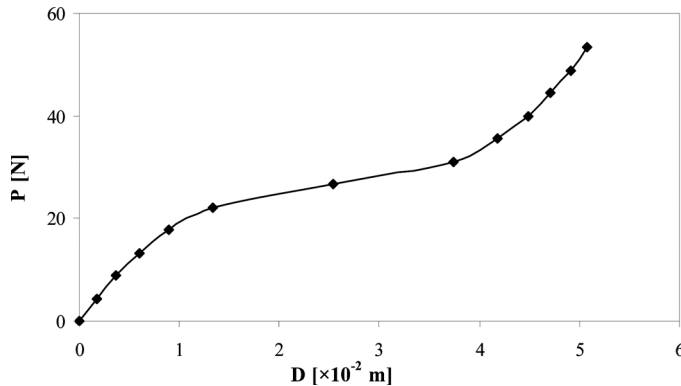


Figure 7 Load-deflection curve for truss-spring system.

Table 2 The number of iterations for convergence in the truss-spring

Meth.	Number of iterations for each load increment												Improvement (%)		
	1	2	3	4	5	6	7	8	9	10	11	12	Total	$\frac{\text{CFT-REMT}}{\text{CFT}}$	$\frac{\text{MFT-REMT}}{\text{MFT}}$
CFT	76	73	77	83	95	134	75	57	49	45	42	40	846	91.3	7.5
MFT	5	5	7	7	9	15	8	6	6	4	4	4	80		
REMT	5	5	7	7	7	9	8	6	6	4	4	4	74		

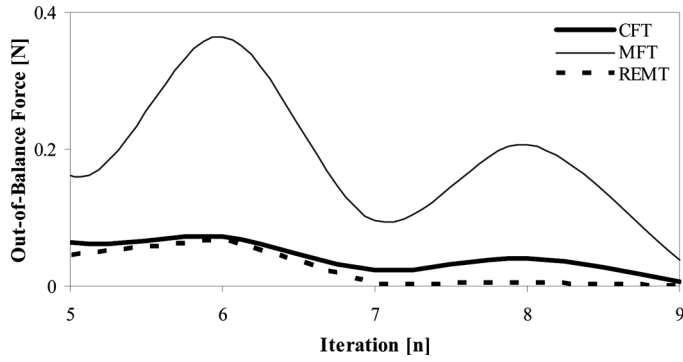


Figure 8 Variation of out-of-balance force for the 12th increment of truss-spring system.

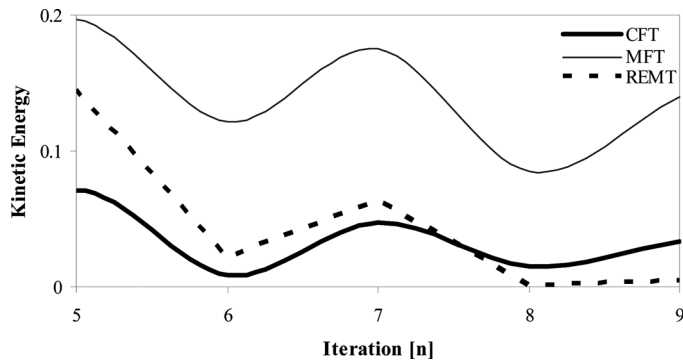


Figure 9 Variation of kinetic energy for the 12th increment of truss-spring system.

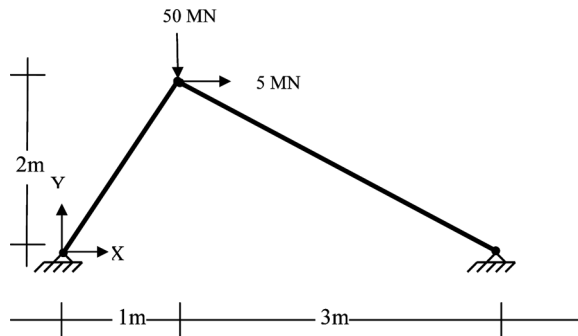


Figure 10 Linear 2D truss.

The result of one increment analysis leads to the horizontal and vertical displacements equal to 6.311 cm and -18.998 cm, respectively. The number of required DR iterations for convergence of the CFT, MFT and REMT is 249, 46 and 35, respectively. It is clear that the proposed method (REMT) gives a reduction

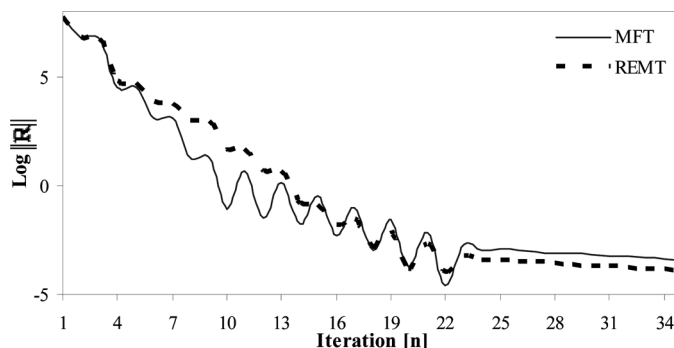


Figure 11 Variation of out-of-balance force for the linear 2D truss in logarithmic scale.

up to 23% to 85% compared with the MFT and CFT procedures, respectively. To give more insights, Figs. 11 and 12 show the variations of the residual force and kinetic energy in the logarithmic scale. Based on these figures, one can see that the positive influence of the suggested REMT method appears in the mid of iterations, and in some initial iterations (between 1 and 14), the MFT and REMT schemes are approximately the same. As a result, the overall convergence rate of the REMT is better than the MFT.

Building Frame

A building frame with five bays and six stories is shown in Fig. 13. A uniform load of $q = 50 \text{ kg/cm}$ is applied on each floor and the horizontal forces are calculated by distribution of the base shear arising from an earthquake loading. The columns of three lower and upper stories are constructed from $W18 \times 40$ and $W18 \times 35$, respectively, and all beams are $W16 \times 31$. Small and large deformation analyses are performed for this structure, and co-rotational finite element formulation is utilized for large deformation analysis (Fellippa, 1997). The conventional linear stiffness matrix of the 2D frame element was used for small deflection analysis. Figure 14 demonstrates the load-deflection curves for

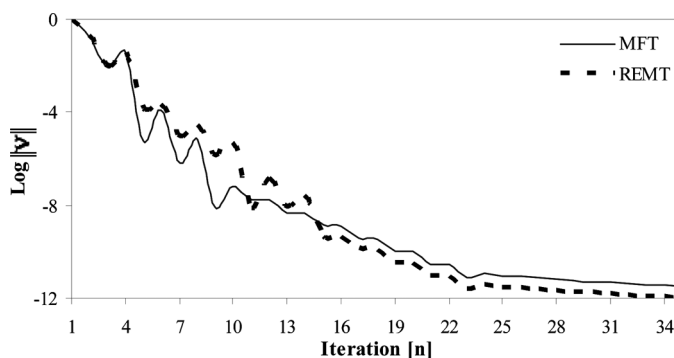


Figure 12 Variation of kinetic energy for the linear 2D truss in logarithmic scale.

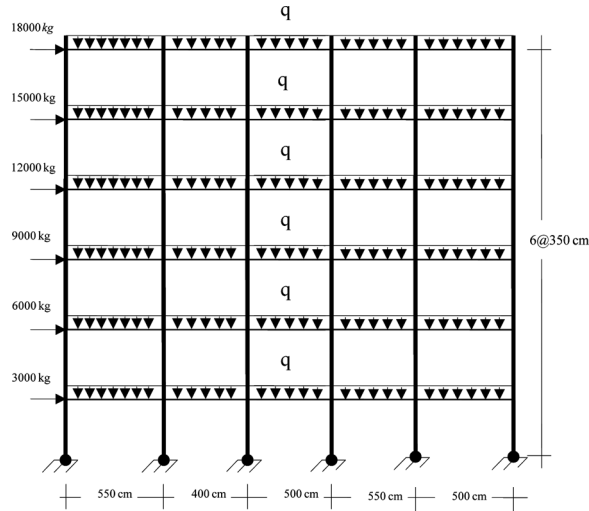


Figure 13 Building frame.

the horizontal displacement of top of the frame for both linear and nonlinear analyses. In the elastic large deflection (nonlinear) analysis this frame has a softening behavior. The number of required iterations for convergence has also been inserted in Table 3. Using the REMT method, a considerable reduction of calculation time up to about 40% may be observed. Calculation of the internal force vector and stiffness matrix is an expensive part of nonlinear analyses, and therefore, reduction of the number of iterations may decrease the cost and the computational time considerably. As a result, using the suggested formulation can be advised for nonlinear, multi degrees of freedom finite element problems like frames. The variations of the unbalance force and kinetic energy for iterations between 600 and 700 have been illustrated by Figs. 15 and 16 for the 10th increment of nonlinear analyses, respectively. These figures also show the preference of new proposed algorithms so that local fluctuations do not appear in the REMT.

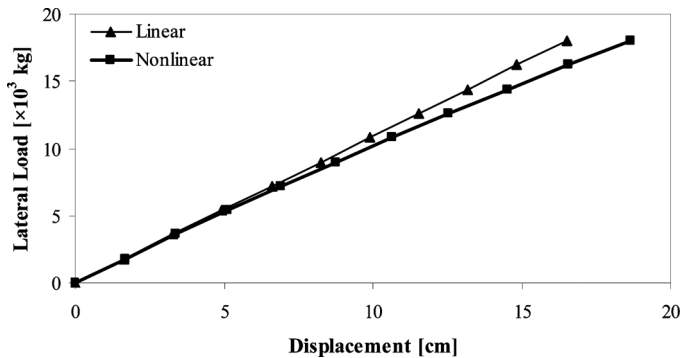


Figure 14 Load-deflection curves of building frame.

Table 3 The number of iterations for convergence in the building frame

Analysis	Meth.	Number of iterations for each load increment										Improvement (%)		
		1	2	3	4	5	6	7	8	9	10	Total	$\frac{\text{CFT-REMT}}{\text{CFT}}$	$\frac{\text{MFT-REMT}}{\text{MFT}}$
Linear	CFT	2090	1626	1585	1568	1559	1554	1550	1547	1545	1543	16,167	44.9	38.9
	MFT	1776	1552	1506	1145	1253	1478	1474	1394	1478	1521	14,577		
	REMT	790	1164	755	862	820	934	850	857	741	1133	8906		
Nonlinear	CFT	2102	1651	1623	1621	1627	1637	1650	1664	1679	1696	16,950	45.9	41.7
	MFT	1786	1443	1527	1491	1570	1608	1607	1589	1490	1618	15,729		
	REMT	604	791	773	926	834	1275	912	964	1178	915	9172		

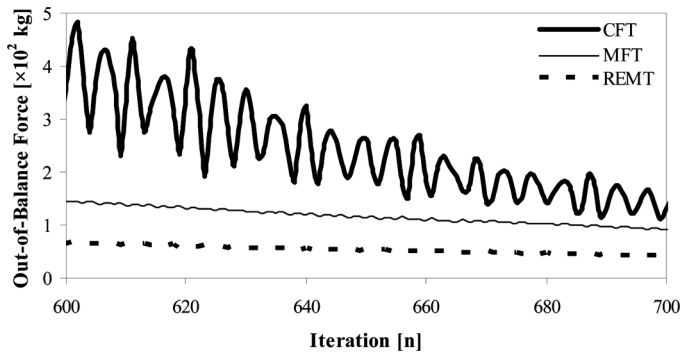


Figure 15 Variation of out-of-balance force for the 10th increment of non-linear building frame.

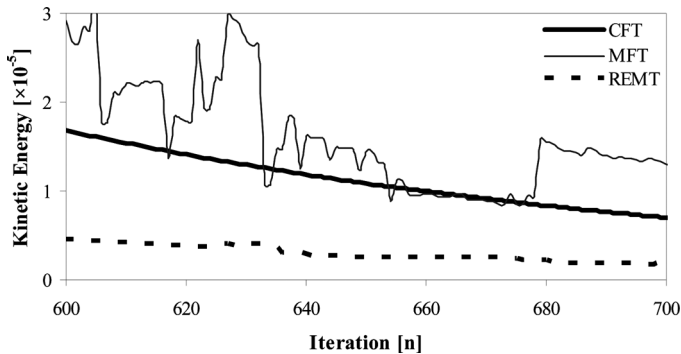


Figure 16 Variation of kinetic energy for the 10th increment of non-linear building frame.

It is also worth emphasizing that the frame structures have different kinds of degrees of freedom such as rotation and transformation. These degrees of freedom and their corresponding internal forces have different numerical units. In the minimum unbalance force algorithm (MFT), the effects of all degrees of freedom are considered to be the same; hence, the effect of different dimensions is not considered and the utility of MFT approach may be decreased. In the REMT algorithm, each element of the unbalance force vector is multiplied by the corresponding residual displacement. This procedure causes dimensional consistency of different degrees of freedom. Hence, the ability and also the efficiency of the suggested method increase. In addition, the effect of nonhomogenous degrees of freedom is limited and higher efficiency may be achieved in the intense nonlinearities. The results of building frame and other wide ranges of the numerical studies which have different types of degrees of freedom prove this merit.

Spherical Cap

Figure 17 shows a clamped spherical cap under a uniformly distributed load (Teng and Rotter, 1989). The thickness of this axisymmetric shell is 1.27 cm. The modulus of elasticity and Poisson's ratio of the purely elastic material are

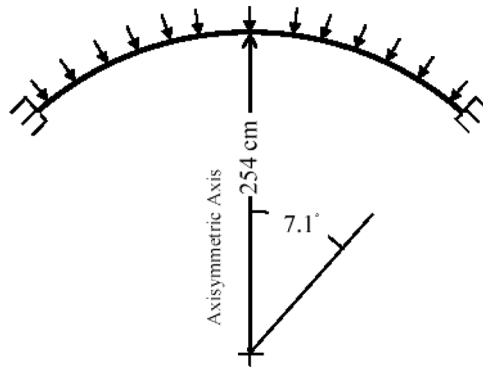


Figure 17 Spherical cap under a uniformly distributed load.

$206.8324 \times 10^6 \text{ N/m}^2$ and 0.3, respectively. The finite element analysis of this thin-walled structure is based on total Lagrangian formulation of axisymmetric shells (Oliver and Onate, 1986). This formulation allows for large displacements and large rotations of the structures. Moreover, shear deformation effects have also been taken into account. Here, three axisymmetric shell elements are used. The loading process is completed during eight increments with a total load of $8,277,300 \text{ N/m}^2$. Figure 18 shows the load versus displacement at the apex. This structure has both softening and hardening behaviors. The number of required iterations for convergence has been inserted in Table 4. In this case, a maximum reduction up to 25% and 7%, in comparison to the MFT and CFT algorithms, may be obtained. On the other hand, Figs. 19 and 20 demonstrate variations of the out-of-balance force and kinetic energy for the 4th increment, respectively (between iteration 300 and 400). These figures also confirm the effectiveness of REMT compared to MFT and CFT methods.

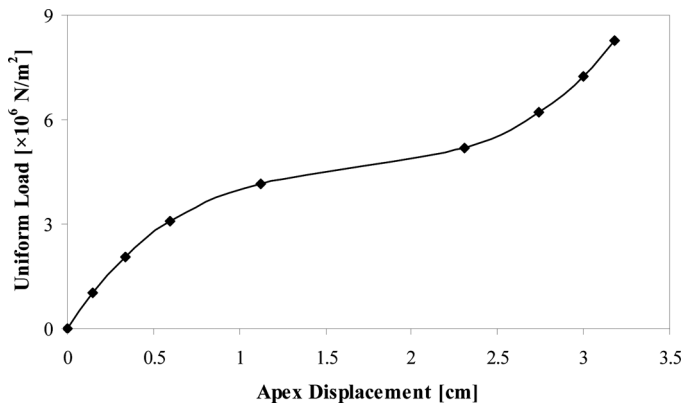


Figure 18 Load-deflection curve for the spherical cap.

Table 4 The number of iterations for convergence in the spherical cap

Meth.	Number of iterations for each load increment								Total	Improvement (%)	
	1	2	3	4	5	6	7	8		<u>CFT-REMT</u>	<u>MFT-REMT</u>
										CFT	MFT
CFT	49	55	66	102	113	65	54	49	5562	26.9	7.7
MFT	2	1	0	5	8	5	9	2	4403		
REMT	1	5	3	5	37571	0					
REMT	28	36	43	84	96	48	34	34	4065		
	1	5	7	1	2	6	7	6			

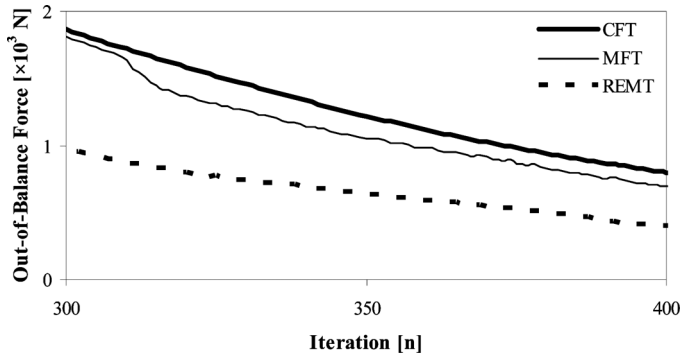
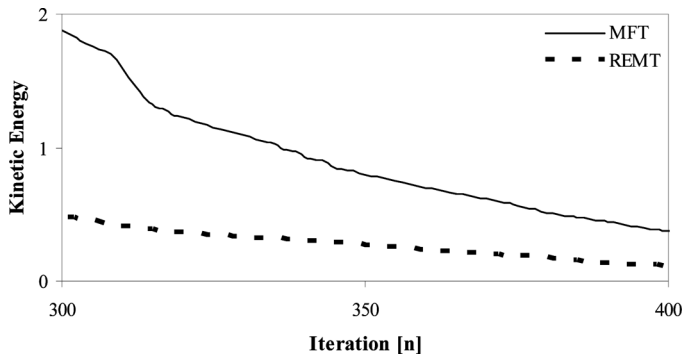
**Figure 19** Variation of out-of-balance force for the 4th increment of the spherical cap.**Figure 20** Variation of kinetic energy for the 4th increment of the spherical cap.

Plate Structures with Finite Differences Analysis

A plate with a general configuration as shown in Fig. 21 is analyzed under uniform pressure (q). This plate is constructed from steel with modulus of elasticity $2E6 \text{ kg/cm}^2$ and Poisson ratio of 0.3. The dimensions a , b and h are assumed to be 150 cm, 100 cm and 0.8 cm, respectively. Other sizes, such as c_1 , c_2 , d_1 and d_2 , will be determined for each analysis. In this example, finite differences analysis of the plate bending is performed by numerical solution of the differential equilibrium

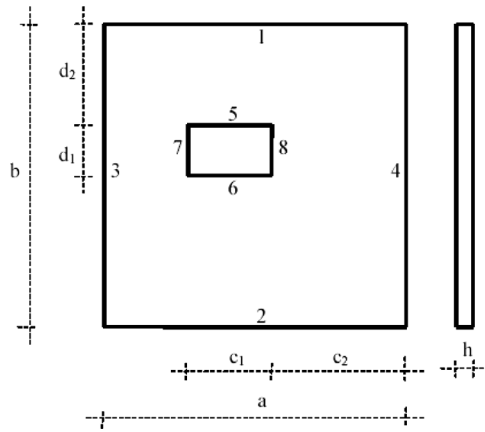


Figure 21 Geometry of plate structure for finite differences analysis.

equations. The equilibrium equations of the structure can be written as follows, (Kadkhodayan et al., 1997),

$$\begin{aligned} \frac{\partial N_x}{\partial x} + \frac{\partial N_{xy}}{\partial y} &= 0 \\ \frac{\partial N_y}{\partial y} + \frac{\partial N_{xy}}{\partial x} &= 0 \\ \frac{\partial^2 M_x}{\partial x^2} + \frac{\partial^2 M_y}{\partial y^2} - 2 \frac{\partial^2 M_{xy}}{\partial x \partial y} + N_x \frac{\partial^2 w}{\partial x^2} + N_y \frac{\partial^2 w}{\partial y^2} + 2N_{xy} \frac{\partial^2 w}{\partial x \partial y} + q &= 0, \end{aligned} \tag{36}$$

where the internal forces are defined as below,

$$(N_x, N_y, N_{xy}, M_x, M_y, M_{xy}) = \int_{-h/2}^{h/2} (\sigma_x, \sigma_y, \tau_{xy}, z\sigma_x, z\sigma_y, z\tau_{xy}) dz \tag{37}$$

The stresses are related to the strains by Hooke's law and the strains can be written in the following,

$$\varepsilon_x = \varepsilon_x^0 + z\kappa_x, \quad \varepsilon_y = \varepsilon_y^0 + z\kappa_y, \quad \gamma_{xy} = \gamma_{xy}^0 + z\gamma_{xy} \tag{38}$$

The mid-plane strains and curvatures may be written as functions of displacements,

$$\begin{aligned} \varepsilon_x^0 &= \frac{\partial u}{\partial x} + \frac{1}{2} \left(\frac{\partial w}{\partial x} \right)^2, \quad \varepsilon_y^0 = \frac{\partial v}{\partial y} + \frac{1}{2} \left(\frac{\partial w}{\partial y} \right)^2, \quad \gamma_{xy}^0 = \frac{\partial u}{\partial y} + \frac{\partial v}{\partial x} + \frac{\partial w}{\partial x} \frac{\partial w}{\partial y} \\ \kappa_x &= -\frac{\partial^2 w}{\partial x^2}, \quad \kappa_y = -\frac{\partial^2 w}{\partial y^2}, \quad \kappa_{xy} = 2 \frac{\partial^2 w}{\partial x \partial y} \end{aligned} \tag{39}$$

The above relationships show the large deflection behavior of plates. As mentioned, the finite difference method is utilized for the analysis and the numbers of mesh

Table 5 Comparison between the numerical and analytical results for a uniformly loaded rectangular plate ($c = d = 0$)[$a/b = 1.5$]

Case	Boundary conditions along edges				Deformation type	$\frac{12qb^4(1-\nu^2)}{Eh^4}$	$\frac{w_{max}}{h}$		Error % $\frac{(w_{max})_N - (w_{max})_A}{(w_{max})_A} \times 100$
	1	2	3	4			Analytical	Numerical	
R1	C	C	C	C	L.D.*	1000	1.20	1.2073	+0.6
R2	C	C	C	C	L.D.	500	0.8	0.8096	+1.2
R3	S	S	C	C	S.D.**	500	2.655	2.6618	+0.3
R4	S	S	C	F	S.D.	50	0.5274	0.5155	-2.3
R5	S	S	S	F	S.D.	50	0.5226	0.5317	+1.7

*Large deformation. **Small deformation.

intervals used in the computation were 20, 20, and 11 for the length, width and thickness directions, respectively. For rectangular plates ($c_1 = d_1 = 0$), the numerical results of the DR method have been compared with the analytical solution (Timoshenko and Woinowsky-Krieger, 1959) in Table 5 and the accuracy of the numerical results is almost acceptable.

Furthermore, plates with a rectangular hole have been analyzed under uniform pressure with large deflection behavior. The geometrical and loading specifications, boundary conditions and the obtained results have been inserted in Table 6. Also symbols C, S, F, RP and PP indicate the clamped edge, simply support, free edge, rectangular plate ($c_1 = c_2 = d_1 = d_2 = 0$) and punched plate ($2c_1/3 = c_2 = d_1 = d_2 = 30$ cm), respectively. The results indicate that when the REMT is used the average reductions in iterations compared with the MFT and CFT algorithms are about 10% and 18%, respectively. In order to observe the differences between the convergence rates of different DR algorithms more clearly, the variation of the out-of-balance force and the kinetic energy at each iteration has been studied. These quantities show how the dynamic response diminishes as the solution is approached. For this purpose, cases with a mixture of boundary conditions, i.e. RP2 and PP1, have been selected (see the Table 6). The results are illustrated in Figs. 22–25. Because the differences between the results are more significant during the initial iterations, the differences between the out-of-balance force and kinetic energy are shown for a part of iterations. It is observed that using REMT method reduces the unbalance force faster than the conventional methods. Moreover, it can be easily seen that the kinetic energy obtained with the use of the REMT method is always lower than that with the MFT. Although some small fluctuations take place when using this method, the total number of iterations is always less than the conventional schemes (Figs. 22 and 23). In other words, some local oscillations do not have any significant effect on the improvement made by the REMT procedure.

CONCLUSION

In this paper, a REMT is formulated for the DR method by minimizing the unbalance energy function in each iteration. To assess the proposed technique, the modified fictitious timestep (MFT) and the constant fictitious timestep (CFT) were

Table 6 The number of iterations for convergence in the punched plate structures

Plate	Boundary conditions								Converged iterations				Improvement (%)		
	1	2	3	4	5	6	7	8	$\frac{12\alpha b^4(1-\nu^2)}{Eh^4}$	$\frac{w_{max}}{h}$	CFT	MFT	REMT	$\frac{CFT-REMT}{CFT}$	$\frac{MFT-REMT}{MFT}$
RP1	C	C	C	C	-	-	-	-	500	0.8096	644	634	542	15.8	14.5
RP2	S	S	S	S	-	-	-	-	400	1.045	1177	1011	949	19.4	6.1
RP3	C	S	F	S	-	-	-	-	250	0.7752	1045	882	747	28.5	15.3
PP1	C	S	F	S	S	S	S	S	500	1.1380	762	659	610	19.9	7.4
PP2	C	S	S	S	S	F	C	S	1000	0.9133	496	495	456	8.1	7.9
PP3	C	S	F	S	S	F	C	C	1000	1.5473	841	826	706	16.1	14.5

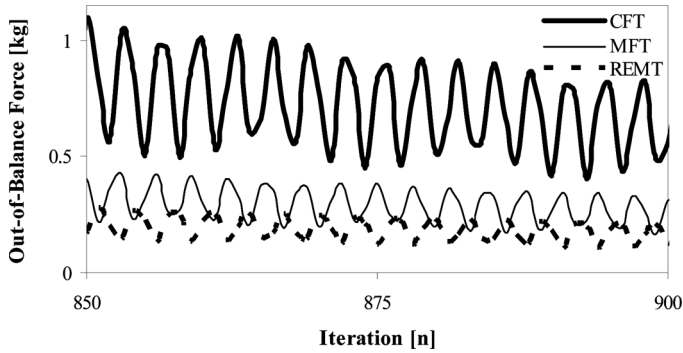


Figure 22 Variation of out-of-balance force of the plate RP2.

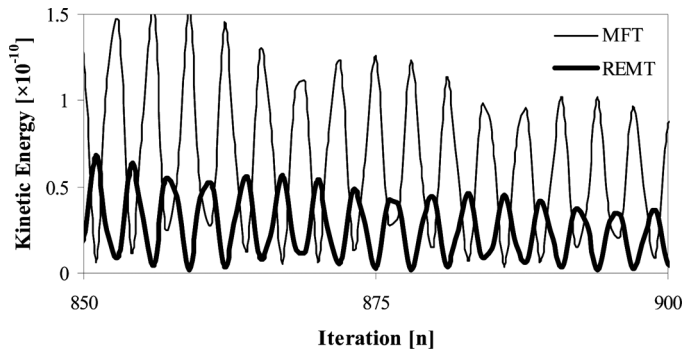


Figure 23 Variation of kinetic energy of the plate RP2.

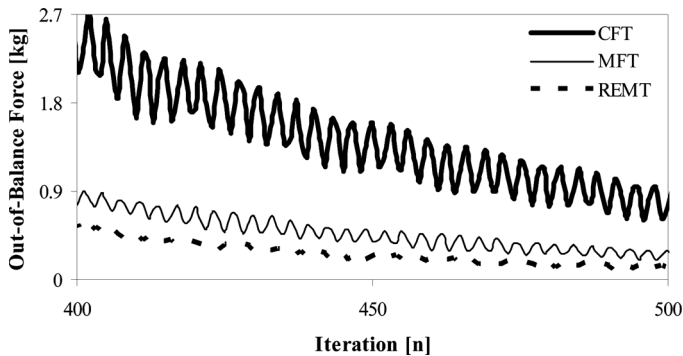


Figure 24 Variation of out-of-balance force of the plate PPI.

utilized. The mathematical convergence rank of DR algorithm for a single degree of freedom system demonstrates that both REMT and MFT tactics improve the convergence rank from one to infinity for linear problems. However, these schemes promote the convergence rank from one to two for nonlinear analysis. Moreover, the ability of REMT algorithm was investigated for both finite difference (small

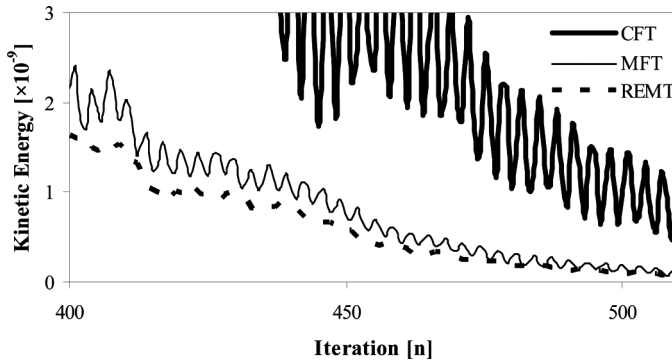


Figure 25 Variation of kinetic energy of the plate PP1.

and large deflections of plate bending problems with different boundary conditions) and finite element problems (truss, frame and thin-walled structures with elastic geometrically nonlinear behavior).

The numerical results show that the proposed formulation (REMT) has an appropriate efficiency in both finite elements and finite differences solutions. In the analysis of plate bending problems by the finite difference strategy, the average reduction in the number of iterations is up to about eighteen and eight percent in comparison to the CFT and MFT algorithms, respectively. On the other hand, these reductions are twenty eight and eight percent in finite element analysis, respectively. It can be concluded that the proposed algorithm has a good efficiency in both finite element and finite difference methods and does not depend on any formulation scheme. Hence, the suggested technique can be most probably used in other kinds of engineering problems. Moreover, the developed fictitious time does not impose any additional convergence criteria and, at the same time, it optimizes the convergence rate of the DR method, especially in the initial stage of the iterative procedure.

APPENDIX: THE MATHEMATICAL CONVERGENCE RATE

For a simple structure with only one degree of freedom Eqs. (15) and (27) take the same form, as follows,

$$\tau_{REMT} = \tau_{MFT} = \frac{r^n}{f^{n+\frac{1}{2}}} \tag{A.1}$$

Mathematically, it is known that the ability of an iterative method to yield converged results depends on the magnitude of its convergence rank. One of the conventional methods for determining the convergence rank uses Taylor series. In this method, the degree of the first nonzero derivative in the iterative relation is usually identified as the convergence rank (Murphy et al., 1988), as shown in the following relation,

$$\varepsilon^{n+1} = \varepsilon^n g'(\alpha) + \frac{(\varepsilon^n)^2}{2!} g''(\alpha) + \dots + \frac{(\varepsilon^n)^m}{m!} g^{(m)}(\alpha) + \dots , \tag{A.2}$$

where the quantities α and ε^n are the real solution and the error in the n th iteration, respectively ($D^n = \alpha + \varepsilon^n$). The function (g) also is determined from the characteristics of the solution process, and can be written as,

$$D^{n+1} = g(D^n). \quad (\text{A.3})$$

In the following, the convergence rank of the DR method for the cases of constant (CFT), modified (MFT), and REMT is determined. First, the iterative function (g) is formulated from equations (3) and (4) in the following form,

$$g(D) = D + \tau^{n+1} \left[\frac{2 - c^n \tau^n}{2 + c^n \tau^n} v^{n-\frac{1}{2}} + \frac{2\tau^n}{(2 + c^n \tau^n)m^n} r^n \right], \quad (\text{A.4})$$

where the mass and damping quantities may be substituted from Eqs. (7) and (8), respectively. Now, for a one degree of freedom system, these quantities can be simplified as follows,

$$\begin{cases} m^n = \frac{S_T(\tau^n)^2}{4} \\ c^n \tau^n = 4\sqrt{\frac{S_G}{S_T}} \end{cases} \quad (\text{A.5})$$

where S_T and S_G are the tangent and secant stiffness, respectively. Initially, the fictitious time is assumed to be constant and equal to unity for all nodes and all iterations. In this case, the function g_1 becomes

$$g_1(D) = D + \frac{\left(2 - 4\sqrt{\frac{S_G}{S_T}}\right)v^{n-\frac{1}{2}} + \frac{8r^n}{S_T}}{2 + 4\sqrt{\frac{S_G}{S_T}}}. \quad (\text{A.6})$$

Using the MFT and REMT (Eq. A.1), leads to the following iterative function g_2 ,

$$g_2(D) = D + \frac{r^n}{S_T}. \quad (\text{A.7})$$

Now, the first derivative of functions g_1 and g_2 with respect to the displacement can be found as follows,

$$g'_1(\alpha) = 1 + \frac{8}{2 + 4\sqrt{\frac{S_G}{S_T}}} \left[1 - \frac{\left(S_T \frac{\partial S_G}{\partial D} - S_G \frac{\partial S_T}{\partial D}\right) \sqrt{\frac{S_T}{S_G}} v^{n-\frac{1}{2}}}{(S_T)^2 \left(2 + 4\sqrt{\frac{S_G}{S_T}}\right)} \right] \neq 0 \quad (\text{A.8})$$

$$g'_2(D) = -\frac{r^n \frac{\partial S_T}{\partial D}}{(S_T)^2} \Big|_{\alpha} = 0 \quad (\text{A.9})$$

Here, primes denote the derivative respect to the displacement. Because of the nonzero first derivative for the function g_1 , the convergence rank of the DR method

Table 1-A The convergence rank of the DR method

Convergence rank	Fictitious timestep	
	Nonlinear	Linear
1	1	CFT
∞	2	MFT
∞	2	REMT

with a constant fictitious time will be equal to unity. On the other hand, the second derivative of g_2 has the following form,

$$g_2''(D) = - \frac{r^n \left[\frac{\partial^2 S_T}{\partial D^2} S_T - 2 \left(\frac{\partial S_T}{\partial D} \right)^2 \right] - (S_T)^2 \frac{\partial S_T}{\partial D}}{(S_T)^3} \bigg|_{\alpha} = \frac{\frac{\partial S_T}{\partial D}}{S_T} \bigg|_{\alpha} \quad (A.10)$$

In general, the relation (A.10) is not zero; hence, the convergence rank of the DR method using MFT and REMT for the nonlinear problems will be equal to two. However, the tangent stiffness remains constant during the analysis for linear problems and the following equation can be written,

$$\frac{\partial S_T}{\partial D} = \frac{\partial^2 S_T}{\partial D^2} = \dots = \frac{\partial^m S_T}{\partial D^m} = \dots = 0. \quad (A.11)$$

Therefore, from Eqs. (A.10) and (A.11), the second derivative of g_2 in linear problems is zero, and it is easy to show that all of the subsequent derivatives for linear problems will be equal to zero. Thus, it can be concluded that the convergence rank of the DR method with the modified fictitious timestep and REMT is infinite for linear problems. Table 1-A gives a summary of the convergence ranks of the DR method for conventional (CFT), modified (MFT), and REMT for the systems with one degree of freedom.

NOMENCLATURE

- $A_1^{n+1}, A_2^{n+1}, A_3^{n+1}$ formulation parameters in $n + 1$ th increment
- AE axial rigidity
- \mathbf{A}^n artificial acceleration vector in n th iteration
- c^n artificial damping factor in n th iteration
- \mathbf{C}^n artificial damping matrix in n th iteration
- DOF number of degrees of freedom
- \mathbf{D} vectors of displacement
- EI flexural rigidity
- \mathbf{f} vector of internal forces
- $\dot{\mathbf{f}}$ vector of internal force increment
- \mathbf{M}^n artificial mass matrix in n th iteration

P	vector of external loads
UEF	unbalance energy function
UFF	unbalance force function
R	vector of unbalance force
S	stiffness matrix
Vⁿ	artificial velocity vector in <i>n</i> th iteration
CFT	constant fictitious time
MFT	modified fictitious time
REMT	residual energy minimizer timestep
<i>Superscripts</i>	
<i>n</i>	iteration number of DR method
<i>Subscripts</i>	
<i>i</i>	each degree of freedom of structure

REFERENCES

- Alwar, R. S., Rao, N. R., Rao, M. S. (1975). Alternative procedure in dynamic relaxation. *Computers and Structures* 5:271–274.
- Bardet, J. P., Proubet, J. (1991). Adaptive dynamic relaxation for statics of granular materials. *Computers and Structures* 39:221–229.
- Brew, J. S., Brotton, M. (1972). Non-linear structural analysis by dynamic relaxation method. *International Journal for Numerical Methods in Engineering* 3:463–483.
- Bunce, J. W. (1972). A note on estimation of critical damping in dynamic relaxation. *International Journal for Numerical Methods in Engineering* 4:301–304.
- Cassell, A. C., Hobbs, R. E. (1976). Numerical stability of dynamic relaxation analysis of non-linear structures. *International Journal for Numerical Methods in Engineering* 10:1407–1410.
- Cassell, A. C., Kinsey, P. J., Sefton, D. J., Wood, W. L., (1968). Cylindrical shell analysis by dynamic relaxation. *Proc. Inst. Civ. Engrs.* 39:75–84.
- Day, A. S. (1965). An introduction to dynamic relaxation. *The Engineer* 219:218–221.
- Domer, B., Fest, E., Lalit, V., Smith, I. F. C. (2003). Combining dynamic relaxation method with artificial neural networks to enhance simulation of tensegrity structures. *ASCE, Journal of Structural Engineering* 129(5):672–681.
- Felippa, C. A. (1982). Dynamic relaxation under general increment control. *Math. Prog.* 24:103–133.
- Felippa, C. A. (1997). *Nonlinear Finite Element Methods (ASEN 5017)*, Course Material, Colorado University, Bouldes, CO.
- Frankel, S. P. (1950). Convergence rates of iterative treatments of partial differential equations. *Mathematical Tables and Other Aids to Computation* 4(30):65–75.
- Frieze, P. A., Hobbs, R. E., Dowling, P. J. (1978). application of dynamic relaxation to the large deflection elasto-plastic analysis of plates. *Computers and Structures* 8:301–310.
- Han, S. E., Lee, K. S. (2003). A study on stabilizing process of unstable structures by dynamic relaxation method. *Computers and Structures* 80:1677–1688.
- Kadkhodayan, M., Alamatian, J., Turvey, G. J. (2008). A new fictitious time for the dynamic relaxation (DXDR) method. *International Journal for Numerical Methods in Engineering* 74:996–1018.

- Kadkhodayan, M., Zhang, L. C. (1995). A consistent DXDR method for elastic-plastic problems. *International Journal for Numerical Methods in Engineering* 38:2413–2431.
- Kadkhodayan, M., Zhang, L. C., Swerby, R. (1997). Analysis of wrinkling and buckling of elastic plates by DXDR method. *Computers and Structures* 65:561–574.
- Murphy, J., Ridout, D., McShane, B. (1988). *Numerical Analysis Algorithms and Computation*. New York: Ellis Horwood Limited.
- Oliver, J., Onate, E. (1986). A total lagrangian formulation for the geometrically nonlinear analysis of structures using finite elements: Part II: Arches, frames and axisymmetric shells. *International Journal for Numerical Methods in Engineering* 23:253–274.
- Otter, J. R. H. (1966). Dynamic relaxation. *Proc. Inst. Civ. Engrs.* 35:633–656.
- Papadrakakis, M. (1981). A method for automatic evaluation of the dynamic relaxation parameters. *Computer Methods in Applied Mechanics and Engineering* 25:35–48.
- Pasqualino, I. P., Estefan, S. F. (2001). A nonlinear analysis of the buckle propagation problem in deepwater pipelines. *International Journal for Solids and Structures* 38:8481–8502.
- Qiang, S. (1988). An adaptive dynamic relaxation method for non-linear problems. *Computers and Structures* 30:855–859.
- Ramesh, G., Krishnamoorthy, C. S. (1993). Post-buckling analysis of structures by dynamic relaxation. *International Journal for Numerical Methods in Engineering* 36:1339–1364.
- Ramesh, G., Krishnamoorthy, C. S. (1994). Inelastic post-buckling analysis of truss structures by dynamic relaxation method. *International Journal for Numerical Methods in Engineering* 37:3633–3657.
- Rezaiee-Pajand, M., Alamatian, J. (2008a). Nonlinear dynamic analysis by dynamic relaxation method. *Journal of Structural Engineering and Mechanics* 28(5):549–570.
- Rezaiee-Pajand, M., Alamatian, J. (2008b). Implicit higher order accuracy method for numerical integration in dynamic analysis. *Journal of Structural Engineering ASCE* 134(6):973–985.
- Rezaiee-Pajand, M., Alamatian, J. (2010). The dynamic relaxation method using new formulation for fictitious mass and damping. *Journal of Structural Engineering and Mechanics* 34(1):109–133.
- Rezaiee-Pajand, M., Alamatian, J. (2011). Automatic DR structural analysis of snap-through and snap-back using optimized load increments. *Journal of Structural Engineering ASCE* 137(1):109–116.
- Rezaiee-Pajand, M., Kadkhodayan, M., Alamatian, J., Zhang, L. C. (2011). A new method of fictitious viscous damping determination for the dynamic relaxation method. *Computers and Structures* 89(9–10):783–794.
- Rushton, K. R. (1968). Large deflection of variable thickness plates. *International Journal of Mechanical Science* 10:723–735.
- Saka, M. P. (1990). Optimum design of pin-jointed steel structures with practical applications. *Journal of Structural Engineering, ASCE* 116:2599–2619.
- Shawi, F. A. N., Mardirosion, A. H. (1987). An improved dynamic relaxation method for the analysis of plate bending problems. *Computers and Structures* 27:237–240.

- Teng, J. G., Rotter, J. M. (1989). Elastic-plastic large deflection analysis of axisymmetric shells. *Computers and Structures* 31(2):211–233.
- Timoshenko, S., Woinowsky-Krieger, S. (1959). *Theory of Plates and Shells*. New York: McGraw-Hill Book Company.
- Turvey, G. J., Salehi, M. (1990). DR large deflection analysis of sector plates. *Computers and Structures* 34:101–112.
- Turvey, G. J., Salehi, M. (2005). Annular sector plates: Comparison of full-section and layer yield prediction. *Computers and Structures* 83:2431–2441.
- Underwood, P. (1983). Dynamic Relaxation, In: Belytschko, T., Hughes, T. J. R., eds. *Computational Method for Transient Analysis: Computational Methods in Mechanics*. Vol. 1. Chapter 5. Amsterdam: Elsevier Science Publishers, pp. 245–256.
- Welsh, A. K. (1967). Discussion on dynamic relaxation. *Proc. Inst. Civ. Engrs.* 37:723–750.
- Wood, R. D. (2002). A simple technique for controlling element distortion in dynamic relaxation form-finding of tension membranes. *Computers and Structures* 80:2115–2120.
- Wood, W. L. (1971). Note on dynamic relaxation. *International Journal for Numerical Methods in Engineering* 3:145–147.
- Zhang, L. C., Yu, T. X. (1989). Modified adaptive dynamic relaxation method and its application to elastic-plastic bending and wrinkling of circular plates. *Computers and Structures* 34:609–614.
- Zhang, L. C., Kadkhodayan, M., Mai, Y. W. (1994). Development of the maDR Method. *Computers and Structures* 52:1–8.
- Zienkiewicz, O. C., Lohner, R. (1985). Accelerated relaxation or direct solution future prospects for FEM. *International Journal for Numerical Methods in Engineering* 21:1–11.